



HAL
open science

Emergence of Chirality in Hexagonally Packed Monolayers of Hexapentyloxytriphenylene on Au(111): A Joint Experimental and Theoretical Study

Piotr Slezkowski, Nathalie Katsonis, Oleksiy Kapitanchuk, Alexandr Marchenko, Fabrice Mathevet, Bernard Croset, Emmanuelle Lacaze

► **To cite this version:**

Piotr Slezkowski, Nathalie Katsonis, Oleksiy Kapitanchuk, Alexandr Marchenko, Fabrice Mathevet, et al.. Emergence of Chirality in Hexagonally Packed Monolayers of Hexapentyloxytriphenylene on Au(111): A Joint Experimental and Theoretical Study. *Langmuir*, 2014, 30 (44), pp.13275-13282. 10.1021/la5030058 . hal-01206967

HAL Id: hal-01206967

<https://hal.science/hal-01206967>

Submitted on 29 Sep 2015

HAL is a multi-disciplinary open access archive for the deposit and dissemination of scientific research documents, whether they are published or not. The documents may come from teaching and research institutions in France or abroad, or from public or private research centers.

L'archive ouverte pluridisciplinaire **HAL**, est destinée au dépôt et à la diffusion de documents scientifiques de niveau recherche, publiés ou non, émanant des établissements d'enseignement et de recherche français ou étrangers, des laboratoires publics ou privés.

Emergence of chirality in hexagonally packed monolayers of hexapentyloxytriphenylene on Au(111): a joint experimental and theoretical study

Piotr Slezkowski,^{†,‡,§} Nathalie Katsonis,[§] Oleksiy Kapitanchuk,¹ Alexandr Marchenko,[±] Fabrice Mathevet,[#] Bernard Croset,^{†,‡} and Emmanuelle Lacaze,^{*†,‡}*

[†] CNRS UMR7588, Institut des Nano-Sciences de Paris (INSP), Paris, France

[‡] UPMC Univ Paris 06, UMR 7588, Institut des Nano-Sciences de Paris (INSP) Paris, France

[§] Laboratory for Biomolecular Nanotechnology, MESA+ Institute for Nanotechnology, University of Twente, Enschede, The Netherlands ¹ Bogolyubov Institute for Theoretical Physics, National Academy of Sciences of Ukraine, Kiev, Ukraine

[±] Institute of Physics, National Academy of Sciences of Ukraine, Kiev, Ukraine

[#] UPMC Univ Paris 06, UMR 8232, Institut Parisien de Chimie Moléculaire, Equipe Chimie des Polymères, Paris, France

ABSTRACT

We investigate the unusual expression of chirality in a monolayer formed spontaneously by 2,3,6,7,10,11-pentyloxytriphenylene (H5T) on Au(111). We resolve its interface morphology by combining scanning tunnelling microscopy (STM) with theoretical calculations of intermolecular and interfacial interaction potentials. We observe two commensurate structures. While both of them belong to a hexagonal space group, analogical to the triangular symmetry of the molecule and the hexagonal symmetry of the substrate surface, they surprisingly reveal a 2D chiral character. The corresponding breaking of symmetry arises for two reasons. First it is due to the establishment of a large molecular density on the substrate, which leads to a rotation of the molecules with respect to the molecular network crystallographic axes to avoid steric repulsion between neighboring alkoxy chains. Second it is due to the molecule-substrate interactions, leading to commensurable large crystallographic cells associated with the large size of the molecule. As a consequence, molecular networks disoriented with respect to the high symmetry directions of the substrate are induced. The high simplicity of the intermolecular and molecule/substrate Van der Waals interactions leading to these observations suggests a generic character for this kind of symmetry breaking. We demonstrate that, for similar molecular densities, only two kinds of molecular networks are stabilized by the molecule-substrate interactions. The most stable networks favors the interfacial interactions between terminal alkoxy tails and Au(111). The metastable ones favors a specific orientation of the triphenylene core with its symmetry axes collinear to the Au<110>. This specific orientation of the triphenylene cores with respect to Au(111) appears associated with an energy advantage larger by at least 0.26 eV with respect to the disoriented core.

INTRODUCTION

It is well known that a number of achiral molecules adsorbed on crystalline substrates can form 2D chiral structures.^{1,2} This emergence of 2D chirality corresponds to a symmetry breaking induced by interactions with the substrate underlying the molecular monolayers. However, in the large majority of 2D systems reported to date, the chiral domains remain of limited extension and mirror image domains are formed. Therefore the surface-monolayer

system remains racemic at the macroscopic scale. More recently a number of studies evidenced the possibility to favor specific 2D monolayers chiral plane groups, either by using chiral solvents,^{3,4} a sergeant-and-soldiers approach^{3,5-7} or chiral auxiliaries.⁸⁻¹¹ As a consequence, a precise understanding of how the interplay between molecule/substrate and molecule/molecule interactions allows the emergence of extended chiral domains in 2D, becomes of primary importance. Many STM investigations concerning supramolecular chirality at the liquid/solid interface have focused either on the influence of the substrate¹ or on the influence of specific molecule/molecule interactions, for example hydrogen bonding,¹²⁻¹⁷ or covalent bonding [humblot]. Some antiferromagnetic-like coupling between molecules has also been demonstrated.¹⁸ One system however displayed chirality for simple steric and Van der Waals molecule-substrate and molecule-molecule interactions, HtB-HBC on Cu(110). [Richardson, Joachim]

Here, we confirm that the balance between steric and Van der Waals molecule/substrate and intermolecular interactions can promote the formation of 2D chiral domains, thanks to the necessity for the molecular system to increase its density on the substrate. This is shown for 2,3,6,7,10,11-hexapentyloxytriphenylene (H5T), a model (archetypal) molecule - composed by an aromatic core that is symmetrically substituted by six alkoxy chains containing five carbons each. This achiral molecule presents a 3-fold symmetry, analogical to the 6-fold symmetry of the underlying gold surface. Upon self-assembly, a hexagonal network is formed, leading to an STM contrast without any sign of chirality.¹ However, using the observation of metastable domains by STM, together with calculations of steric Van der Waals interactions between molecules, we establish the symmetry breaking associated with the presence of two kinds of domains, a stable and a metastable one. Analyzing the molecular orientations within the two domains, we demonstrate that the Au(111)/triphenylene core interaction is more favorable for a specific orientation of

the core, close to be parallel to the Au<110> direction and is responsible for the appearance of the metastable domains. We estimate the corresponding energetic advantages and reveal the induced chirality of the two domains. The observation of density-driven symmetry breaking with simple symmetric molecules suggests that a large number of physisorbed molecules are likely to present a similar behavior.

EXPERIMENTAL

The Au(111) substrate was purchased from Neyco, and consisted of 150 nm gold layer evaporated onto mica support. Annealing with a gas flame (propane-air) was performed until signs of glowing appeared on the sample. 2,3,6,7,10,11-hexapentyloxytriphenylene (H5T) has been synthesized and characterized within the Laboratoire de Chimie des Polymères, Université Pierre et Marie Curie (Paris, France). Additional purification by the column chromatography has been performed, and material from several batches has been used for further studies. H5T is a discotic liquid crystal that exhibits a hexagonal columnar mesophase in bulk between 69°C and 122°C.¹⁹ H5T was dissolved in *n*-tetradecane (Sigma Aldrich, pure >99%, used as received) with a concentration of 1.67 mmol/L. The solution was heated up to ~70°C for 15 min prior to deposition onto freshly flame-annealed gold. A 50 µL droplet of this solution was deposited onto the gold substrate. Two kinds of depositions were performed onto Au(111) substrates. One was onto hot substrate, at 100°C, the second one onto cold substrate, at ambient temperature. The STM tip was mechanically cut from a Pt/Ir wire (90/10 wt%, GoodFellow Inc.) and was immersed in the droplet after cooling back, for the scanning process. The structures of monolayers were investigated using Bruker-multimode 5A with low-current head. Typical imaging conditions in constant current mode were 100-500 mV for the tip voltage and 5-50 pA for the tunnelling current. All STM imaging was carried out at room temperature.

RESULTS

Figures 1b and 1c represent typical STM images recorded following the deposition of H5T/*n*-tetradecane droplet on heated ($T = 100 \pm 1$ °C) Au/mica sample, just after flame-annealing the substrate²⁰. Bright spots are clearly organized into hexagonal mesh. In accordance to the well-known fact of strong contribution of aromatic motifs to the STM contrast,²¹ we infer that those bright spots resemble the central triphenylene cores. Moreover, it should be noticed that all molecular rows are aligned along the $\langle 110 \rangle$ crystallographic direction of Au(111), since they form 30° angle with the gold reconstruction, this latter one being featured by yellow dashed-lines on Figure 1. The fact that Au(111) reconstruction is not lifted as a result of the monolayer formation suggests that the discotic molecules are physisorbed. Lack of any periodic variation of STM contrast within the observed monolayers suggests that the physisorption has occurred at energetically equal adsorption sites. This situation was preserved throughout subsequent scans, for different scanning directions, tip-sample polarities and tunnelling current parameters. The value of distance between two nearest neighbors, equal 2.0 ± 0.1 nm, is obtained from the analysis of STM images. The molecular rows being oriented along $\langle 110 \rangle$, this value must be compared to the corresponding Au(111) period, equal to 0.288 nm. This leads to the conclusion that the distance between two neighboring H5T molecule is equal to seven times the distance between two gold atoms along the $\langle 110 \rangle$ crystallographic direction of Au(111). It is worth noticing that the observed period value of 2 nm is very close to the bulk columnar period of the liquid crystal phase²¹ and thus the 2D monolayer presents a compactness comparable to the bulk one. This latter characteristics appears in contrast with the H5T 2D monolayers on graphite, which display smaller period than the bulk one.¹⁸

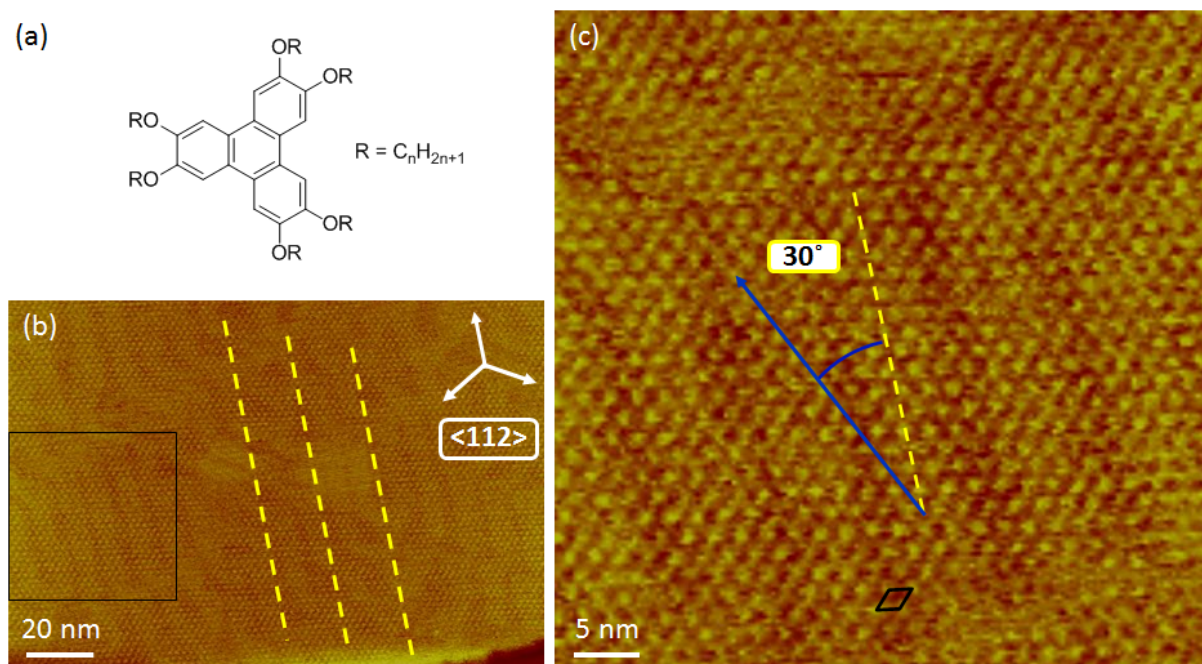


Figure 1. (a) Schematic representation of hexakis-2,3,6,7,10,11-alkoxytriphenylene, a molecule belonging to the D_{3h} point-symmetry group. (b) and (c) STM images of H5T molecules self-assembled at the n -tetradecane/Au(111) interface. Yellow dashed-lines highlight the main direction of Au(111) reconstruction, i.e. the $\langle 112 \rangle$ directions. Black square at (b) represents the zoomed area shown in (c). Black diamond at (c) represents the primitive unit cell of H5T monolayer physisorbed at Au(111); $I_t = 5$ pA, $V_t = 100$ mV.

The schematic representation of the packing of H5T molecular nodes at n -tetradecane/Au(111) interface is illustrated by the blue hexagonal mesh on Figure 2, and may be denoted by (7×7) according to Woods terminology. We call it in the following $M0$ mesh (Table 1).

Surprisingly, when deposition of H5T/ n -tetradecane solution is performed onto a cold substrate, i.e. not directly after its flame-annealing, STM images also reveal that another type

of domain usually coexists with (7×7) domains on Au(111). The situation is depicted by Figure 3, where (7×7) domain areas (A), and the ‘cold-deposition’ domain areas (B) are emphasized by blue and red lineaments, respectively. A detailed study of the lateral distances between triphenylene cores in A and B areas provides a value of 2.0 ± 0.1 nm for the periodicity of lattice nodes in both kinds of domains. As in the previous case, no sign of periodic variation of STM contrast of probed self-assemblies is observed suggesting commensurability of both A and B domains. Drift-corrected image analysis resulted in determination of the angle between respective unit vectors of A and B unit cells: $14 \pm 1^\circ$. Taking into account all geometrical features of B-type domains obtained from STM measurements, one may construct a model that theoretically corresponds to the observed unit cell. The hexagonal mesh of the 2D crystal presented on Figure 2 with a red color corresponds to the second type of domain found after ‘cold-deposition’. Its theoretical nearest neighbor distance value equals 2.077 nm, with the unit cell vectors rotated by 13.9° from previously found (7×7) domain. It may be denoted as $(\sqrt{52} \times \sqrt{52})R13.9^\circ$ in Woods terminology (*M3* mesh-table 1). Comparison of Figure 3a and Figure 3b obtained on the same sample evidences the two possible orientation of *M3* domains, 13.9° and -13.9° .

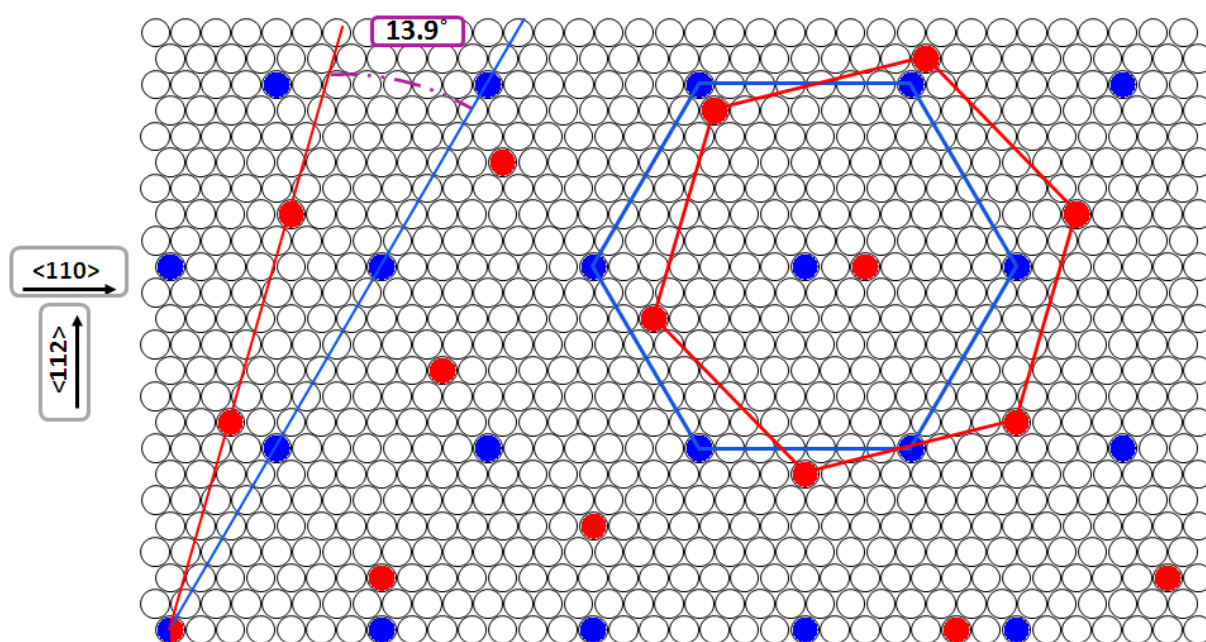


Figure 2. Proposed model of packing of H5T at a *n*-tetradecane/Au(111) interface for (7 x 7) and ($\sqrt{52} \times \sqrt{52}$) $R13.9^\circ$ domains, indicated by a blue- and a red-color mesh, respectively.

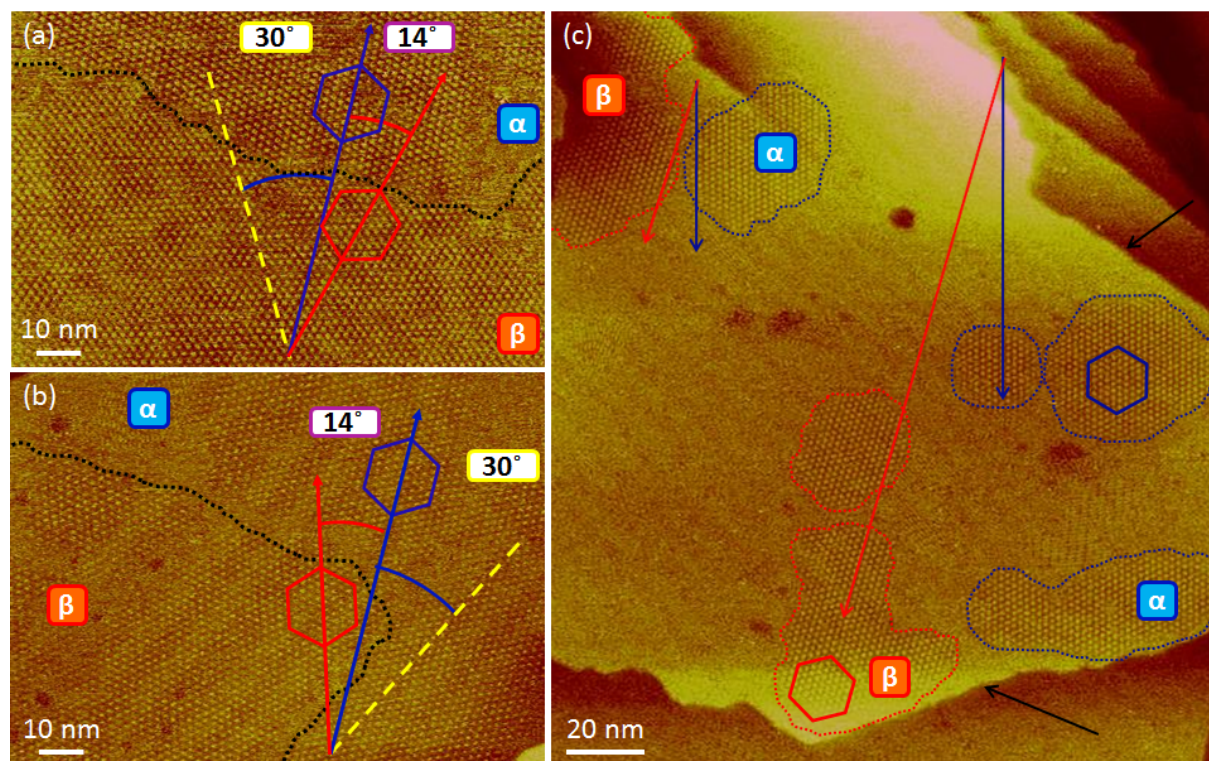


Figure 3. STM images of twofold orientation of H5T molecules self-assembled at the *n*-tetradecane/Au(111) interface. (7 x 7) domains (A) and ($\sqrt{52} \times \sqrt{52}$) $R13.9^\circ$ domains (B) are depicted by blue and red graphics, respectively. Yellow dashed-lines at (a) and (b) highlight the main direction of Au(111) reconstruction, i.e. the $\langle 112 \rangle$ directions, black dotted-lines at (a) and (b) highlight the domain boundaries. (a) and (b) STM pictures are taken on the same Au(111) monocrystal and evidence the two possible orientations of (B) domains, at $\pm 13.9^\circ$ from the (A) ones. Black arrows at (c) show the step-edges of Au(111) substrate, parallel to the α -domains dense directions which confirm an orientation along $\langle 110 \rangle$ for the (7 x 7) mesh; $I_t = 10$ pA, $V_t = 100$ mV.

Knowing that the two-dimensional crystals formed by the H5T mesogens are commensurate does not give clear view on the driving force behind the self-assembly process, since no information can be obtained concerning the mutual orientation of the molecules within the monolayer or with respect to the surface. It should be recalled that physisorbed self-assemblies find their origin in the subtle interplay between intermolecular and interfacial interactions. Due to the structural dichotomy of H5T, one may expect competition between its two components: the triphenylene core and the pentyloxy chains, since they are likely to display different relative affinities to the substrate.²³ The obstacle in analysis of H5T monolayers on Au(111) results from the fact that molecules are visualized as blurred spots, as soon as the scale that normally should enable intramolecular resolution is attained. In particular alkoxy chains are never visible, in connection with their mobility despite the fact that they may also present a well-defined average location on the substrate.

We have thus used theoretical calculations to provide further insight into the geometry of the system. We have started by considering a single molecule to estimate the orientation of alkoxy chains in average with respect to the central triphenylene core. Figure 4 represents the optimized geometry of an isolated H5T molecule calculated by Density Functional Theory (DFT/B3Lyp/6-31G*). As may be noticed H5T retains its tri-fold symmetry and central triphenylene core, as expected for polyconjugated moiety, remains flat. What should be further perceived is that each of the three equivalent sides of the triphenylene motif remains in the plane of the central part of the molecule, but is associated with two alkoxy chains bent apart by approximately $15 \pm 1^\circ$. This minimized energy conformation will serve us as a model molecular structure for the physisorbed monolayers.

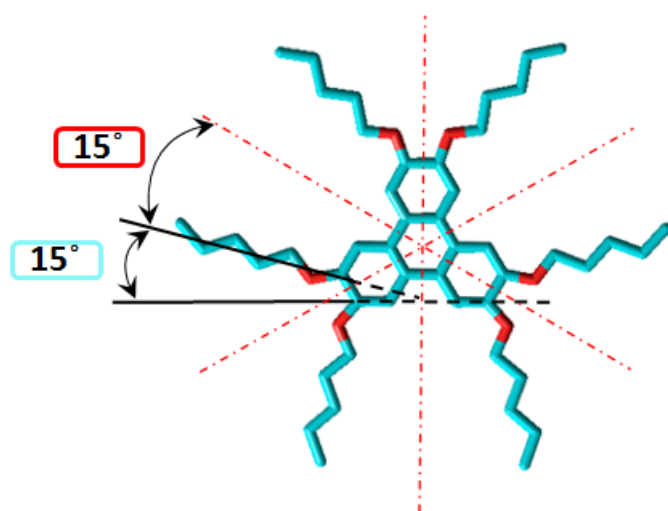


Figure 4. Optimized geometry of H5T molecule calculated by Density Functional Theory (DFT/B3LYP/6-31G*). Red dash-dotted lines that represent symmetry axes of molecule underline its affiliation to the D_{3h} symmetry group. The planar character of the molecule is well noticeable, with an important alkoxy chains deflection by 15° from the respective symmetry axis.

DISCUSSION

In addition to the commensurability of the monolayer, for our investigations we have made two main assumptions. On one hand, molecules tend to maximize their packing density (together with alkyl chains lying flat on the surface) and thus minimize the adsorption energy of the system. On the other hand, we need to take into account the steric repulsion between each building block associated with the peripheral alkoxy parts.

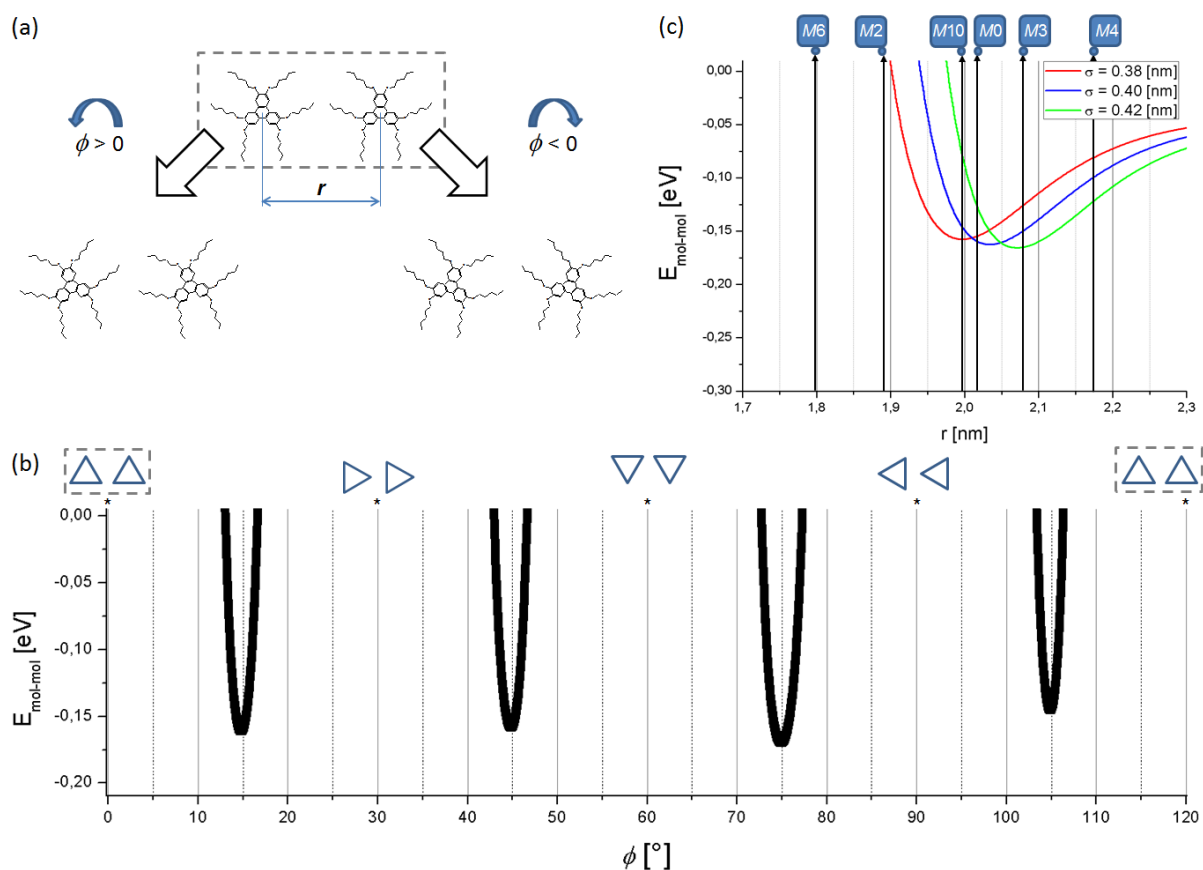


Figure 5. Two H5T molecules with parallel directions and their schematic unidirectional in-plane rotation of angle $\pm\phi$. r stands for the distance between the centers of their masses (varying for different meshes, see: Table 1). (b) Angular dependence of the Lennard-Jones intermolecular energy of interaction ($E_{\text{mol-mol}}$) for the dimers shown at Figure 5a with 7×7 ($M0$) mesh parameter (i.e. $r = 2.016$ nm). Since H5T belongs to $p6m$ symmetry group energetically allowed regions appear periodically and exhibit a mirror symmetry about each $(2k + 1) \cdot 30^\circ$ value (k being an integer). Pairs of blue triangles show symbolically the orientation the corresponding aromatic cores (angles marked with asterisks). (c) Lennard-Jones intermolecular interactions as a function of intermolecular distance, r , for different values of σ parameter, ϕ being optimized for each r . Lack of the non-negative part of the plot enables to exclude $M6$ and $M2$ meshes (table 1) from further considerations.

We start with the intermolecular interaction, $E_{\text{mol-mol}}$ and consider a pair of molecules uniformly oriented in one plane (as depicted on the top of Figure 5a) with a separation distance between centers of their masses, r , the lattice parameter. Possessing exact atomic coordinates, it is possible, by summing the Lennard-Jones (12-6 LJ) potential between each methylene group of the alkyl chains, to calculate the interaction between two molecules and probe the evolution of this interaction for unidirectional in-plane rotation of a molecular couple (Figure 5a). The Lennard-Jones potential between two methyl group is $E_{\text{LJ}} = 4 \epsilon [(\sigma/d)^{12} - (\sigma/d)^6]$, $\epsilon = 10.3 \text{ meV}$ and $\sigma = 0.398 \text{ nm}$ from Ref.²⁴. Angular dependence of this interaction is presented on the Figure 5b for (7 x 7) mesh. The energetically allowed range (i.e. $E < 0$), appears as a rather narrow angular region which strictly defines the molecule orientation in the reference mesh. The interaction value, of the order of 0.15 eV appears of the same order but smaller than the interaction between Au(111) and a $\langle 110 \rangle$ -oriented C_5 -carbon chain, equal to -0.53 eV ²⁵, suggesting that the attractive molecular interactions do not dominate the molecule/substrate interactions. Taking into account the value, $\phi_t^0 = 13.6^\circ$, corresponding to the energy minimum, and the alkoxy chain deflection by 15° from the molecule's symmetry axis, we obtain, that three out of six $-\text{C}_5\text{H}_{11}$ chains of each H5T molecule would be roughly oriented parallel to the Au $\langle 110 \rangle$. It is well known that $\langle 110 \rangle$ is the preferred crystallographic direction for physisorption of alkanes on Au(111).²⁶⁻²⁸ Alkyl chains may thus strongly contribute to the adsorption energy of (7 x 7) domains. This result evidences the unexpected chirality of the (7 x 7) mesh, associated with the rotation around $\pm 13.6^\circ$ of the molecule with respect to the Au $\langle 110 \rangle$ direction. This is in the same time a point and an organizational chirality, the molecules being disoriented with respect to the 2D array as well. This chirality, in other word the $\pm 13.6^\circ$ rotation of the molecule, could not be detected through the STM contrast only due to the "invisibility" of the alkoxy chains. It appears of very different nature with respect to the chirality demonstrated for the same

molecules adsorbed on HOPG, this latter one being associated with different adsorption geometry of one molecule out of two.¹⁸

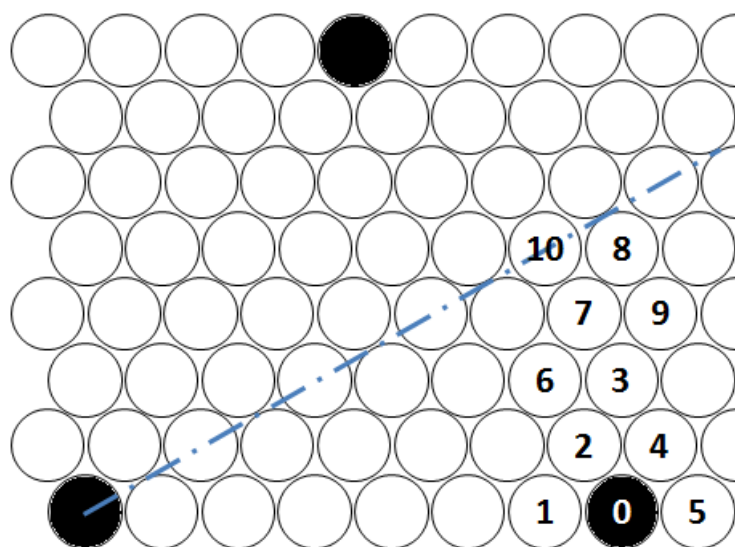


Figure 6. Schematic representation of the reference (7 x 7) structure (black atomic sites, M_0). Alternative meshes ($M_1 \dots M_{10}$) are created on the basis of a unit vector of absolute value close to the one of the (7 x 7) mesh. Each mesh is hooked at the center of the atom in the left-bottom corner and spans to the respective atomic site (numbered). Blue dash-dotted line points the mirror symmetry axis.

Alternative two-dimensional commensurate hexagonally packed meshes with near cell parameters must be considered. Altogether with the (7 x 7) reference mesh, that will be denoted M_0 hereafter, we denote these structures M_1, \dots, M_{10} , according to numbered atomic sites shown on Figure 6. All of the characteristics of the constructed set of meshes, including the lattice parameter, are summarized in Table 1. The metastable $(\sqrt{52} \times \sqrt{52})R13.9^\circ$ structure (M_3) appears slightly less dense than M_0 . Computations of Lennard-Jones interactions are shown on Figure 5c, for molecule-molecule distances varying between 1.7 nm and 2.3 nm

according to the variation of cell parameter from $M0$ to $M10$ (Table 1), ϕ being optimized for each r . The phenomenological parameter σ was allowed to take three different values: 0.38, 0.40 and 0.42 nm. Figure 5c shows that steric considerations exclude clearly structure $M1$, $M6$ and that for $M2$ structure not to be excluded, the σ value must be equal to 0.38 nm, *i.e.* significantly lower than the standard value 0.398 nm. At this stage, we exclude $M1$, $M6$ and $M2$ structures for steric reasons and $M4$, $M8$, $M9$ and $M5$ structures because their low surface densities lead to a remarkable loss in molecule-surface interactions. Figure 7a reveals an important result, the value of the angle ϕ_i^0 around 14° determined by steric consideration is common to all the structures, this result being robust with respect to σ variations. Like $M0$, the $M10$, $M3$ and $M7$ meshes exhibit molecule disorientation around 14° with respect to the crystallographic axis of the mesh. This finally leads to the same organizational chirality for all these structures. All of the ϕ_i^0 values for meshes considered in further investigations are indicated in Table 1, together with the triphenylene core orientation with respect to the substrate, represented by β . $\beta = 0^\circ$ stands for molecular symmetry axes (see Figure 4) pointing along Au<112>.

Table 1. Comparison of 2D model lattices illustrated on Figure 6, *with their relative surface density with respect to the thermodynamically stable (7 x 7) mesh ($M0$). †Final orientations of the central triphenylene cores are presented with respect to Au<110> crystallographic direction of substrate ($\beta = 0^\circ$ stands for molecular symmetry axes (see Figure 4) pointing along Au<112>). For each mesh its corresponding angular value of interaction energy minimum (ϕ_i^0) is also considered, except for the sterically forbidden ($M1$, $M6$ and $M2$) and low surface-density structures ($M4$, $M8$, $M9$ and $M5$).

Mesh	Lattice parameter r [nm]	Relative surface density*	Mesh rotation angle vs. Au<110> α [°]	Intermolecular rotation minima ϕ_1^0 [°]	Triphenylene orientation†		Alkyl chain orientation vs. Au<110>	
					β [°]			
<i>M1</i>	1.728	1.361	0.0					
<i>M6</i>	1.799	1.256	16.1					
<i>M2</i>	1.889	1.140	7.6					
<i>M10</i>	1.995	1.021	30.0	13.6	16.4	-16.4	1.4	31.4
<i>M0</i>	2.016	[-]	0.0	13.6	13.6	-13.6	-1.4	28.6
<i>M7</i>	2.016	1.000	21.8	13.6	24.6	8.2	-6.8	23.2
<i>M3</i>	2.077	0.942	13.9	13.5	27.4	0.4	-14.6	15.4
<i>M4</i>	2.174	0.860	6.6					
<i>M9</i>	2.286	0.778	19.1					
<i>M5</i>	2.304	0.766	0.0					
<i>M8</i>	2.249	0.803	26.3					

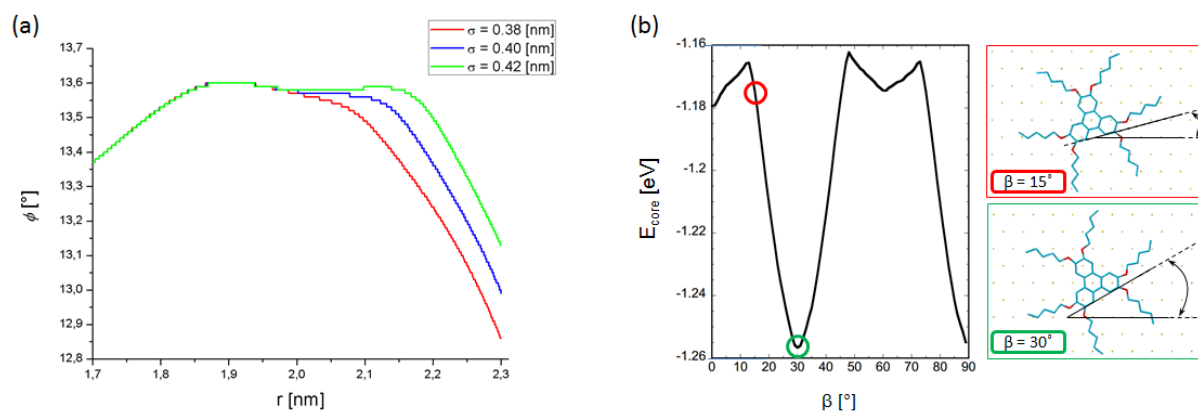


Figure 7. (a) The plot of ϕ_1^0 angle as a function of intermolecular distance, showing robustness with respect to σ variations. (b) Energy plot of molecule-substrate interactions based on a 12-6 LJ potential, as a function of the molecule rotation angle, β (table 1). For this calculation only the central triphenylene core has been taken into consideration (alkoxy tails excluded). Schemes in red and green boxes indicate the actual orientations of the core with respect to the substrate for the $+15^\circ$ and $+30^\circ$ rotations, respectively (the latter one being visibly favorable, since occupying the energetic minimum).

We must now understand the observation of *M0* and *M3* structures together with the non-observation of *M7* and *M10* structures and thus evaluate the variations of molecule/substrate interactions. Table 1 shows that the orientations of the molecules with respect to the substrate are close for *M0* -which is observed- and *M10* -which is not observed- on one hand and for *M3* -which is observed- and *M7* -which is not observed- on the other hand. In the case of *M0* and *M10*, the molecule orientation allows three of the alkoxy chains to be parallel (*M10* case) or almost parallel (*M0* case, misfit angle of 3°) to the Au $\langle 110 \rangle$ direction which is known to be an energetically favorable direction. In contrast, all the six alkoxy chains are misoriented for *M3* and *M7* structures.

In order to evaluate the interaction energy between the triphenylene core and the substrate, E_{core} , we have performed a summation of Lennard-Jones terms between the carbon atoms of the core and the Au atoms of the surface using $\sigma_{\text{C-Au}} = 3.0 \text{ \AA}$ and $\epsilon = 0.013 \text{ eV}$.²⁸ The summation being done for all the distances between interacting atoms superior to $2.5 \sigma_{\text{C-Au}}$. Results are shown on Figure 7b: E_{core} is presented as a function of the core orientation with respect to the substrate, β , the position of the molecule being optimised for each value of this orientation. A strong minimum is observed for $\beta = 30^\circ$. This is consistent with the stabilization of the *M3* structure which is observed despite the non-favourable orientation of the alkyl chains, together with a lower density for *M3* with respect to *M0*. One of the initially allowed β value for *M3* of 0.4° may be finally not observed, as inferred from Figure 7b (Table 1). The other β value is not exactly 30° , but 27.4° . However, the large width of the potential well in Figure 5b (i.e. 4°) authorizes a disorientation between 27.4° and 30° for the *M3* mesh. The value $\beta = 24.6^\circ$ associated with *M7* may appear in contrast too far from the minimum of Figure 7b to allow for the stabilization of *M7* mesh in agreement with experimental non-observations of *M7* by STM. On the other hand, no sensible energy differences in E_{core} are visible on Figure 7b between the orientations corresponding to *M0* and *M10*. The origin of the non-observation of *M10* mesh is thus not clear. We may postulate that the core/Au potential may exhibit rapid variation with β not accounted by our model. This suggests that the flexibility of the molecule should be taken into account to refine the model. Accordingly the numerical values of Figure 7b do not quantitatively describe the experimental data. The potential well at 30° is not deep enough to account for the stabilization of *M3* with a density lower by 6% with respect to *M0*. Taking into account the known energy of adsorption for the $\langle 110 \rangle$ -oriented C_5 -carbon chain, equal to -0.53 eV ,²⁵ together with a ${}^{M0}E_{\text{core}}$ value equal to -1.17 eV (Figure 7b), we would expect ${}^{M3}E_{\text{core}} - {}^{M0}E_{\text{core}}$ to be larger than 0.26 eV , i.e. 3 times more than the calculated potential well.

A major conclusion arising from the scenario depicted above is thus the dual origin of both H5T domains on Au(111), driven by specific interactions of the substrate with either the polyaromatic core or the alkoxy chains and leading to a 2D chirality of both structures. *M0* is associated with organizational chirality but *M3* is chiral as well, whatever corresponding to a different chirality. It is worth noticing that, generally speaking, for large molecules, if the molecule-substrate interactions are strong enough to impose commensurate structure, we expect emergence of point chirality structures. They correspond to meshes disoriented with respect to the dense crystallographic directions of the substrate, which must exist if the intermolecular distance is significantly large with respect to the substrate period. This is here the case of *M10* and *M3*. However, the molecule-substrate interactions being strong enough to impose commensurability, usually it also leads to selection of specific chiral structures among all possible ones, here *M3* only. For one given selected mesh, it also leads to selection of only a limited number of diastereoisomers among the possible ones, as already shown for HtB-HBC on Cu(110).^[Richardson, Joachim] molecules on Cu(111). For *M3*, combining point chirality together with the same chirality than *M0*, four diastereoisomers are expected.^[Richardson, Joachim] We expect clockwise and anticlockwise orientation of the mesh, which are indeed observed as shown on Figure 3. Moreover, for each of these two meshes orientations, as shown in table 1, we would expect a molecular disorientation of $\pm 13.6^\circ$ to fulfil the observed large adsorbed density. However, we finally show that, due to specific triphenylene core-Au(111) interactions, only two diastereoisomers may exist instead of four, corresponding to $\beta = \pm 27.4^\circ$. The *M0* and *M3* chirality, deduced on a basis of twofold orientation of domains consisting of equidistant lattice nodes residing on the surface sites of similar potential, could not be directly evidenced from STM pictures. A theoretical analysis finally appears instrumental in elucidating the chiral character of the structures.

Two meshes over a number of eleven commensurate structures are finally selected: in the first one, M3, the interactions between triphenylene core and substrate are dominating, while the second one, M0, benefits from the stabilizing alkyl chains. We discovered the specificity for the triphenylene core/Au substrate interaction, leading to a favorable interaction for the orientation of the triangular motif of triphenylene core with its apexes pointing the Au<110> directions. For triphenylene molecules with C₅H₁₁ alkyl chains, this latter geometry appears of similar energy to the one with three over six chains oriented parallel to the Au<110>. Consequently our results also suggest that for alkoxy chains shorter than pentyloxy, the core may be oriented parallel to the Au<110> for all molecules. For chains longer than C₅H₁₁, we expect in contrast disoriented triphenylene cores. This finally suggests that increasing the alkoxy chains length would also select only one kind of adsorbed mesh, the latter one. Ultimately (for increasing *n* further), we can even expect that the monolayer loses the hexagonal symmetry, which would definitely allow a larger number of alkoxy chains in epitaxy with respect to Au(111). This last event has been well described previously, with the H11T forming row-like structures on Au(111),^{23, 30} or on graphite for alkoxy chains of length longer than 12 carbons.³¹

CONCLUSIONS

In this article we present a detailed description of the self-assembly of H5T, a discotic molecule, on Au(111). Although H5T and its several homologues have been studied previously on different substrates, here we evidence the emergence of chirality in two structures that coexist in the monolayer. By combining both experimental and theoretical approach we evidence the commensurability of the two structures, respectively (7 x 7) and ($\sqrt{52} \times \sqrt{52}$)R13.9°. Our calculation shows that the maximization of molecular density on the

substrate leads to a rotation of the molecules with respect to the molecular network crystallographic axes to avoid steric repulsion between neighboring alkoxy chains. This rotation plays a major role in the emergence of chirality together with the induced commensurability of the adsorbed molecular structures. For large adsorbed molecules, commensurability implies large structures and therefore potential disorientations of the molecular network with respect to the high symmetry directions of the underlying substrate. Moreover we evidence that the Au(111) substrate stabilizes only few of the potentially allowed adsorbed structures, as a result of the dual nature of interfacial interactions. ($\sqrt{52} \times \sqrt{52}$) $R13.9^\circ$ domains benefit from the triphenylene (aromatic) core interactions with gold while the (7 x 7) structure is stabilized by the three out of six pentyl chains for each molecule. We thus evidence a specifically stabilized orientation for the triphenylene core with its symmetry axes collinear to the Au<110>. This orientation represents an energy advantage at least larger than 0.26 eV with respect to disoriented core. Moreover, we demonstrate that H5T constitutes an interesting example where equilibrated contributions from both aromatic and aliphatic counterparts are present. This appears in contrast with longer peripheral substituents, i.e. for H11T, where alkyl parts dominate the organisation of the monolayer, that is manifested by the hexagonal symmetry breaking.^{23,30}

REFERENCES

- (1) Katsonis, N.; Lacaze, E.; Feringa B. L. Molecular chirality at fluid/solid interfaces: expression of asymmetry in self-organised monolayers. *J. Mater. Chem.* **2008**, *18*, 2065–2073.
- (2) Ernst, K.-H. Supramolecular surface chirality. *Top. Curr. Chem.* **2006**, *265*, 209–252.
- (3) Xu, H.; Ghijsens, E.; George, S. J.; Wolffs, M.; Tomovic, Z.; Schenning, A. P. H. J.; De Feyter, S. Chiral Induction and Amplification in Supramolecular Systems at the Liquid-Solid Interface. *ChemPhysChem* **2013**, *14*, 1583–1590.
- (4) Katsonis, N.; Xu, H.; Haak, R. M.; Kudernac, T.; Tomovic, Z.; George, S.; Van der Auweraer, M.; Schenning, A. P. H. J.; Meijer, E. W.; Feringa, B. L.; De Feyter, S. Emerging Solvent-Induced Homochirality by the Confinement of Achiral Molecules Against a Solid Surface. *Angew. Chem., Int. Ed.* **2008**, *47*, 4997–5001.
- (5) Tahara, K.; Yamaga, H.; Ghijsens, E.; Inukai, K.; Adisoejoso, J.; Blunt, M. O.; De Feyter, S.; Tobe, Y. Control and induction of surface-confined homochiral porous molecular networks. *Nat. Chem.* **2011**, *3*, 714–719.
- (6) Masini, F.; Kalashnyk, N.; Knudsen, M. M.; Cramer, J. R.; Lægsgaard, E.; Besenbacher, F.; Gothelf, K. V.; Linderoth, T. R. Chiral induction by seeding surface assemblies of chiral switches. *J. Am. Chem. Soc.* **2011**, *133*, 13910–13913.

- (7) Parschau, M.; Romer, S.; Ernst, K.-H. Induction of homochirality in achiral enantiomorphous monolayers. *J. Am. Chem. Soc.* **2004**, *126*, 15398–15399.
- (8) De Feyter, S.; Grim, P. C. M.; Rucker, M.; Vanoppen, P.; Meiners, C.; Sieffert, M.; Valiyaveetil, S. Müllen, K.; De Schryver, F. C. Expression of chirality by achiral coadsorbed molecules in chiral monolayers observed by STM. *Angew. Chem., Int. Ed.* **1998**, *37*, 1223–1226.
- (9) De Cat, I.; Guo, Z.; George, S. J.; George, S. J.; Meijer, E. W.; Schenning, A. P. H. J.; De Feyter, S. Induction of chirality in an achiral monolayer at the liquid/solid interface by a supramolecular chiral auxiliary. *J. Am. Chem. Soc.* **2012**, *134*, 3171–3177.
- (10) Zhao, J.-S.; Ruan, Y.-B.; Zhou, R.; Jiang, Y.-B. Memory of chirality in J-type aggregates of an achiral perylene dianhydride dye created in a chiral asymmetric catalytic synthesis. *Chem. Sci.* **2011**, *2*, 937–944.
- (11) Guo, Z.; De Cat, I.; Van Averbeke, B.; Lin, J.; Wang, G.; Xu, H.; Lazzaroni, R.; Beljonne, D.; Meijer, E. W.; Schenning, A. P. H. J.; De Feyter, S. Nucleoside-Assisted Self-Assembly of Oligo (p-phenylenevinylene) s at Liquid/Solid Interface: Chirality and Nanostructures. *J. Am. Chem. Soc.* **2011**, *133*, 17764–17771.
- (12) Samori, P.; Rabe, J. P. Scanning probe microscopy explorations on conjugated (macro) molecular architectures for molecular electronics. *J. Phys.: Condens. Matter* **2002**, *14*, 9955–9973.

- (13) De Feyter, S.; Uji-i, H.; Mamdouh, W.; Miura, A.; Zhang, J.; Jonkheijm, P.; Schenning, A. P. H. J.; Meijer, E. W.; Chen, Z.; Wurthner, F. Schuurmans, N.; Van Esch, J.; Feringa, B. L. Supramolecular chemistry at the liquid/solid interface probed by scanning tunnelling microscopy. *Int. J. Nanotechnol.* **2006**, *3*, 462–479.
- (14) Frommer, J. Scanning tunneling microscopy and atomic force microscopy in organic chemistry. *Angew. Chem., Int. Ed.* **1992**, *31*, 1298–1328.
- (15) Weckesser, J.; De Vita, A.; Barth, J.; Cai, C.; Kern, K. Mesoscopic correlation of supramolecular chirality in one-dimensional hydrogen-bonded assemblies. *Phys. Rev. Lett.* **2001**, *87*, 096101.
- (16) De Feyter, S.; De Schryver, F. C. Two-dimensional supramolecular self-assembly probed by scanning tunneling microscopy. *Chem. Soc. Rev.* **2003**, *32*, 139–150.
- (17) Hermann, B. A.; Scherer, L. J.; Housecroft, C E.; Constable, E. C. Self-Organized Monolayers: A Route to Conformational Switching and Read-out of Functional Supramolecular Assemblies by Scanning Probe Methods. *Adv. Funct. Mater.* **2006**, *16*, 221–235.
- (18) Charra, F.; Cousty, J. Surface-induced chirality in a self-assembled monolayer of discotic liquid crystal. *Phys. Rev. Lett.* **1998**, *80*, 1682–1685.

(Humblot) Humblot, V.; Ortega Lorenzo, M.; Badelley, C. J.; Haq, S.; Raval, R., Local and Global Chirality at Surfaces: Succinic Acid versus Tartaric Acid on Cu(110). *J. Am. Chem. Soc.* **2004**, 126, 6460-6469

(Richardson) Richardson, N. V.; Adsorption-induced chirality in highly symmetric hydrocarbon molecules: lattice matching to substrates of lower symmetry. *New J. Phys.* **2007**, 9, 395

(Joachim) Schöck, M.; Otero, R.; Stojkovic, S.; Hümmelink, F.; Gourdon, A.; Lægsgaard, E.; Stensgaard, I.; Joachim, C.; Besenbacher, F.; Chiral Close-Packing of Achiral Star-Shaped Molecules on Solid Surfaces. *J. Phys. Chem. B Lett.* **2006**, 1001, 12835-12838

(19) Billard, J.; Dubois, J, C.; Tinh, N. H.; Zann, A. Meso phases of disc-like molecules. *Nouv. J. Chim.* **1978**, 2, 535–540.

(20) Slezckowski, P.; Katsonis, N.; Marchenko, A.; Lacaze, E. Two-fold orientation of triphenylene-based discotic liquid crystals on gold. *Mol. Cryst. Liq. Cryst.* **2012**, 558, 1-7.

(21) Fisher, A.; Blöchl, P. Adsorption and scanning-tunneling-microscope imaging of benzene on graphite and MoS₂. *Phys. Rev. Lett.* **1993**, 70, 3263–3266.

(22) Markovitsi, D.; Germain, A.; Millie, P.; Lecuyer, P.; Gallos, L.; Argyrakis, P.; Bengs, H.; Ringsdorf, H. Triphenylene Columnar Liquid Crystals: Excited States and Energy Transfer. *J. Phys. Chem.* **1995**, 99, 1005–1017.

(23) Perronet, K.; Charra, F. Influence of molecular-substrate interaction on the self-assembly of discotic liquid crystals. *Surf. Sci.* **2004**, *551*, 213–218.

(24) Kitaigorodskii, A. I. *Organic Chemical Crystallography*. Consultants Bureau; New York, 1962.

(25) Libuda, J.; Scoles, G. Collision-induced desorption of hydrocarbons physisorbed on Au (111). *J. Chem. Phys.* **2000**, *112*, 1522–1530.

(26) Marchenko, O.; Cousty, J. Molecule length-induced reentrant self-organization of alkanes in monolayers adsorbed on Au (111). *Phys. Rev. Lett.* **2000**, *84*, 5363–5366.

(27) Yamada, R.; Uosaki, K. Two-dimensional crystals of alkanes formed on Au (111) surface in neat liquid: structural investigation by scanning tunneling microscopy. *J. Phys. Chem. B* **2000**, *104*, 6021–6027.

(28) Uosaki, K.; Yamada, R. Formation of two-dimensional crystals of alkanes on the Au (111) surface in neat liquid. *J. Am. Chem. Soc.* **1999**, *121*, 4090–4091.

(29) Yoon, B.; Luedtke, W.; Gao, J.; Landman, U. Diffusion of gold clusters on defective graphite surfaces. *J. Phys. Chem. B* **2003**, *107*, 5882–5891.

(30) Katsonis, N.; Marchenko, A; Fichou, D. Substrate-induced pairing in 2, 3, 6, 7, 10, 11-hexakis-undecalkoxy-triphenylene self-assembled monolayers on Au (111). *J. Am. Chem.*

Soc. **2003**, *125*, 13682–13683.

(31) Wu, P.; Zeng, Q.; Xu, S.; Wang, C.; Yin, S.; Bai, C.-L. Molecular Superlattices Induced by Alkyl Substitutions in Self-Assembled Triphenylene Monolayers. *ChemPhysChem* **2001**, *2*, 750–754.

TOC Graphic (For Table of Contents Only)

